67-FM-46

NATIONAL AERONAUTICS AND SPACE ADMINISTRATION

MSC INTERNAL NOTE NO. 67-FM-46

Outside 11/4-74

APRIL 3, 1967

955 L'Enfant Plaza North, S.W.
Washington, D. C. 20024

COMPARISON OF FIXED-AND VARIABLE-TIME-OF-ARRIVAL GUIDANCE SCHEMES FOR A MARTIAN PROBE LAUNCHED FROM A MANNED FLYBY SPACECRAFT

OCT 30 1968

BY THOMAS B. MURTAGH,
FLORA B. LOWES, AND
VICTOR R. BOND

ADVANCED MISSION DESIGN BRANCH

MISSION PLANNING AND ANALYSIS DIVISION
MANNED SPACECRAFT CENTER
HOUSTON, TEXAS

(NASA-TM-X-69980) COMPARISON OF FIXED AND VARIABLE TIME OF ARRIVAL GUIDANCE SCHEMES FOR A MARTIAN PROBE LAUNCHED FROM A MANNED FLYBY SPACECRAFT (NASA) 54 p

N74-71968

Unclas
00/99 16812

MSC INTERNAL NOTE NO. 67-FM-46

COMPARISON OF FIXED- AND VARIABLE-TIME-OF-ARRIVAL GUIDANCE SCHEMES FOR A MARTIAN PROBE LAUNCHED FROM A MANNED FLYBY SPACECRAFT

By Thomas B. Murtagh, Flora B. Lowes, and Victor R. Bond
Advanced Mission Design Branch

April 3, 1967

MISSION PLANNING AND ANALYSIS DIVISION
NATIONAL AERONAUTICS AND SPACE ADMINISTRATION
MANNED SPACECRAFT CENTER
HOUSTON, TEXAS

Approved: Jack Funk
Jack Funk, Chief
Advanced Mission Design Branch

Approved: John P. Mayer
John P. Mayer, Chief
Mission Planning and Analysis Division

CONTENTS

Section	Page
SUMMARY	1
INTRODUCTION	1
ANALYSIS	2
Reference Trajectories of Probe and Spacecraft	2
Description of Navigation and Guidance Systems	3
Assumptions	4
Description of Simulation	5
DISCUSSION OF RESULTS	5
Navigation Results	5
Spacecraft	6
Probe	8
Guidance Results	8
Spacecraft	9
Probe	11
CONCLUDING REMARKS	13
APPENDIX - SOLUTION FOR THE CONIC TRAJECTORY THAT SATISFIES THE TERMINAL ENTRY CONDITIONS OF v_E, γ_E, h_E	36
REFERENCES	44

TABLES

Table		Page
I	ACCURACY OBTAINED USING ONE MIDCOURSE CORRECTION AND ASSUMING A 300-N. MI. POSITION ERROR AND AN 18-FPS VELOCITY ERROR AT THE MARS SOI	
	(a) Navigation measurements processed at 30-minute intervals	15
	(b) Navigation measurements processed at 15-minute intervals	16
II	ACCURACY OBTAINED USING ONE MIDCOURSE CORRECTION AND ASSUMING A 150-N. MI. POSITION ERROR AND A 9-FPS VELOCITY ERROR AT THE MARS SOI	
	(a) Navigation measurements processed at 30-minute intervals	17
	(b) Navigation measurements processed at 15-minute intervals	18
III	ACCURACY OBTAINED USING TWO MIDCOURSE CORRECTIONS AND ASSUMING A 300-N. MI. POSITION ERROR AND AN 18-FPS VELOCITY ERROR AT THE MARS SOI	
	(a) Navigation measurements processed at 30-minute intervals	19
	(b) Navigation measurements processed at 15-minute intervals	20
IV	ACCURACY OBTAINED USING TWO MIDCOURSE CORRECTIONS AND ASSUMING A 150-N. MI. POSITION ERROR AND A 9-FPS VELOCITY ERROR AT THE MARS SOI	
	(a) Navigation measurements processed at 30-minute intervals	21
	(b) Navigation measurements processed at 15-minute intervals	22

Table | Page

V ACCURACY OBTAINED USING TWO MIDCOURSE CORRECTIONS AND ASSUMING A 75-N. MI. POSITION ERROR AND A 4.5-FPS VELOCITY ERROR AT THE MARS SOI

(a) Navigation measurements processed at 30-minute intervals 23

(b) Navigation measurements processed at 15-minute intervals 24

VI PROBE RMS ΔV SUMMARY COMPARING FTA AND $VTA_{\Delta\gamma_E = 0}$ GUIDANCE WITH AND WITHOUT NAVIGATION AND GUIDANCE CORRECTION IMPLEMENTATION ERRORS 25

FIGURES

Figure		Page
1	Probe and spacecraft reference trajectory geometry	26
2	Geometry of planet-star included angle measurement	27
3	Spacecraft RMS periapsis position uncertainties for measurement intervals of 30 minutes	
	(a) RMS altitude uncertainties at periapsis . .	28
	(b) RMS range uncertainties at periapsis	29
	(c) RMS track uncertainties at periapsis	30
4	Spacecraft RMS periapsis position uncertainties for measurement intervals of 15 minutes	
	(a) RMS altitude uncertainties at periapsis . .	31
	(b) RMS range uncertainties at periapsis	32
	(c) RMS track uncertainties at periapsis	33
5	Probe RMS vacuum periapsis altitude uncertainties for measurement intervals of 30 minutes	34
6	Probe RMS vacuum periapsis altitude uncertainties for measurement intervals of 15 minutes	35

COMPARISON OF FIXED- AND VARIABLE-TIME-OF-ARRIVAL GUIDANCE SCHEMES FOR A MARTIAN PROBE LAUNCHED FROM A MANNED FLYBY SPACECRAFT

By Thomas B. Murtagh, Flora B. Lowes and
Victor R. Bond

SUMMARY

A comparison of fixed- and variable-time-of-arrival guidance schemes for a Mars probe launched from a manned spacecraft during a Mars flyby mission in 1975 is presented. The problem is initiated when the probe and spacecraft separate at the Mars sphere of influence and is terminated when the probe arrives at a specified entry altitude and the spacecraft arrives at periapsis. The relative state between the probe and spacecraft is assumed to be perfectly known so that the uncertainty covariance matrix for the probe is equal to that of the spacecraft. The spacecraft position and velocity uncertainties are reduced by onboard processing of Mars-star included angle measurements using a Kalman filter.

The results of the study indicate that variable-time-of-arrival guidance produces smaller root-mean-square velocity corrections than fixed-time-of-arrival guidance, and would be more advantageous for spacecraft maneuvers. Fixed-time-of-arrival guidance appears to be better for the probe corrections, however, in order to more efficiently control the flight-path angle dispersions at entry.

INTRODUCTION

In reference 1, a preliminary analysis of the probe and spacecraft guidance and navigation systems was presented in which fuel consumption for both vehicles was analyzed as a function of navigation system accuracy, number of navigation measurements processed, dispersions and uncertainties in the trajectory at separation, number and

timing of velocity corrections, and the accuracy of their execution. In this reference, only fixed-time-of-arrival (FTA) position guidance was utilized to compute the root-mean-square (RMS) velocity corrections for both the probe and spacecraft.

The present study may be considered an extension of the analysis presented in reference 1, primarily to compare FTA and variable-time-of-arrival (VTA) guidance for both the probe and spacecraft. The probe is assumed to be separated from the spacecraft at the Mars sphere of influence (SOI) and is constrained to land 1 hour ahead of the spacecraft passage through periapsis.

The purpose of this study, then, is to present the midcourse RMS velocity corrections required for the probe to attain certain flight-path angle dispersions at entry as well as safe vacuum periapsis altitude dispersions and for the spacecraft to attain reasonable altitude dispersions at its periapsis. These RMS corrections are presented for both FTA and VTA guidance. A digital computer program was used to simulate the dynamics of the problem and to process the optical measurements using the Kalman filter.

ANALYSIS

Reference Trajectories of Probe and Spacecraft

The basic geometry of the probe and spacecraft reference trajectories is illustrated in figure 1. The initial position, $\bar{r}_o$, and velocity, $\bar{v}_o$, of the spacecraft on the flyby hyperbola were generated using a matched conic interplanetary program (ref. 2). The probe velocity at the Mars SOI, v_{PROBE}, was computed by specifying the speed at entry, v_E, entry altitude, h_E, and entry flight-path angle, γ_E. The procedure for calculating this velocity is developed in the Appendix. The characteristics of the reference trajectory used for the probe and spacecraft in this study are presented in reference 1 and correspond to the data for $|\bar{v}_o|$ = 27 920 fps in that reference. The results of the analysis represent the uncertainties and dispersions normally distributed about the reference trajectories.

Description of Navigation and Guidance Systems

The navigation system equations employed in this study are identical to those developed in reference 1. The sensitivity vector which relates measurement deviations to state vector deviations for the Mars-star included angle measurement is developed in the same reference. The geometry of the Mars-star included angle measurement is illustrated in figure 2. The appropriate guidance system error equations are also developed in reference 1. The only change in these equations required for the study presented here is in the computation of the guidance matrix, G. This matrix appears in equations B-4 and B-12 of reference 1. Equation B-4 represents the update of the state dispersion covariance matrix X(t) as a result of a guidance maneuver and is written

$$X(t)^{+} = \left[I + G(t)\right] \left[X(t)^{-} - E(t)^{-}\right] \left[I + G(t)\right]^{T} + E(t)^{+} \tag{1}$$

where $(\ )^{+}$ indicates the matrix after the correction and $(\ )^{-}$ represents the matrix immediately prior to the correction.

E(t) is a 6 X 6 matrix of estimation uncertainties and I is a 6 X 6 identity matrix.

Equation B-12 is

$$L(t) = \left[G_1(t)\ G_2(t)\right] \left[X(t) - E(t)\right] \left[G_1(t)\ G_2(t)\right]^{T} \tag{2}$$

where the 6 X 6 guidance matrix G(t) is defined as

$$G(t) = \begin{bmatrix} 0 & 0 \\ G_1(t) & G_2(t) \end{bmatrix} \tag{3}$$

The RMS estimate of the velocity correction is computed from the square root of the trace of equation (2). The guidance matrix, G(t), is computed as a function of the type of guidance to be used (e.g., FTA or VTA). The derivation and discussion of the three types of guidance matrices used in this study are presented in reference 3. The first G(t) matrix developed is for FTA position guidance; the second G(t) matrix developed is for VTA guidance subject to the constraint that the magnitude of the velocity correction be minimized; the third guidance matrix developed is for VTA guidance with the constraint that flight-path angle dispersions at entry are nulled. An alternate derivation for the first two of these guidance matrices is presented in reference 4.

Assumptions

Following are the main assumptions for the study:

1. The probe and spacecraft are separated at the Mars SOI, and the probe is constrained to land 1 hour prior to spacecraft passage through periapsis.

2. At the SOI, the initial spacecraft position and velocity dispersions and uncertainties are assumed equal and are equal to the probe dispersions and uncertainties just prior to separation.

3. The covariance matrix at the time of separation is taken to be diagonal with RMS position and velocity errors equal to 300 n. mi., 18 fps; 150 n. mi., 9 fps; or 75 n. mi., 4.5 fps. The first set of initial errors are considered to be conservative values and the results generated from them can be used for preliminary system design. The second set of initial errors are more realistic and represent values which could be obtained by earth-based tracking of an interplanetary vehicle. The last error set may be optimistic and therefore the results generated from them should be interpreted accordingly.

4. The reference trajectories used are assumed to be ideal conics, and the state transition matrix used to propagate the errors was derived analytically for two-body conic trajectories.

5. The relative state between the probe and spacecraft is perfectly known so that the uncertainty covariance matrix of the probe is equivalent to that of the spacecraft. The spacecraft uncertainty covariance matrix is reduced by processing Mars-star included angle measurements with a Kalman filter.

6. The equation for the total variance of the observation errors, σ_T, can be written as

$$\sigma_T^2 = \sigma_I^2 + (c \tan \theta)^2 \tag{4}$$

and is derived and discussed in reference 1. The parameter σ_I is the standard deviation of the instrument error and was chosen to be 5 arc seconds for this study. The parameter c is defined as the ratio of Mars radius uncertainty to the Mars radius and was taken to be 0.001 in this note. (This value corresponds to a Mars radius error of the order of 2 n. mi.).

7. Both FTA and VTA guidance were used for both the probe and spacecraft. No attempt was made to optimize the velocity correction schedule for either of these types of guidance schemes.

Description of Simulation

A digital computer simulation program, PROBE, developed by the authors was used to generate the results presented in this note. The basic components of this program are a control routine which generates trajectory and covariance matrix time histories for both the probe and spacecraft, a set of subroutines which compute the conic state transition matrix for propagating errors and integrating the state vector along the conic, and another set of subroutines which update the covariance matrices as a result of a navigation measurement or a guidance maneuver. The RMS position and velocity errors, computed from the square root of the trace of the covariance matrices, are presented in a locally-level, coordinate system which displays both in-plane and out-of-plane errors. The x-axis of this coordinate system is along the radius vector to the probe or spacecraft (altitude), the y-axis is in the direction of the velocity (range), and the z-axis is along the orbital angular momentum vector (track). The errors in this system are designated as altitude, range, and track errors, and their time rates of change.

DISCUSSION OF RESULTS

Navigation Results

Uncertainties in the estimate of the state of a vehicle as determined by navigation measurements represent a lower bound for the state dispersions. As can be seen by investigating equation (1), state dispersions are never better than the uncertainties in the estimate. By investigating different navigation systems to reduce the estimate uncertainties, one can expect to also reduce the dispersions. Thus, as the navigation is improved, so is the ability to guide a spacecraft to a specified target.

The navigation for this study was the same as that used in the preliminary Mars probe study of reference 1. That is, the optical measurement considered was the star-planet included angle which was assumed to be measured with an onboard sextant and processed by a Kalman filter.

Mars was at all times the planet used for the measurements. However, the star used for each measurement was randomly chosen from a limited catalogue of stars included in the simulation program. No attempt was made to optimize the choice of stars for the measurements.

For the study presented herein, only one trajectory was used - the trajectory for which $|\bar{v}_o|$ = 27 920 fps. Also for this study, the parameters σ_I and c were assigned the fixed values of 5 arc seconds and 0.001 (approximately 2-n. mi. Mars radius uncertainty), respectively. This trajectory and these value assignments were chosen on the basis of the results and conclusions of a preliminary Mars probe study (ref. 1).

Since the position uncertainty of principle interest is that at periapsis for the spacecraft and at vacuum periapsis for the probe, the results of the analysis are presented for these terminal points only.

Results of the navigation analysis are presented in figures 3, 4, 5, and 6.

Spacecraft.- Figures 3 and 4 show the altitude, range, and track components of spacecraft RMS position uncertainty at Mars periapsis. These values are plotted against time to Mars periapsis in order to illustrate approximately how well the periapsis altitude, range, and track component uncertainties are known at any time along the trajectory. The periapsis altitude for the study was assumed to be 100 n. mi.

Figures 3 and 4 each contain three curves. These three curves represent position uncertainties at Mars periapsis for three different sets of initial RMS position and velocity errors (σ_{R_o} and σ_{v_o}) - that for 300 n. mi., 18 fps; 150 n. mi., 9 fps; and 75 n. mi. 4.5 fps. The results of the latter set of initial errors are presented for information only, as they are considered too optimistic for strictly an onboard navigation system.

From previous studies it has been found that a measurement frequency of less than 15-minute intervals does not significantly affect the periapsis position error curve profile. Thus, the results presented are for measurement intervals of 30 and 15 minutes.

Figure 3 contains resulting data for a measurement interval of 30 minutes. The three RMS position error components - altitude, range, and track - are plotted in figures 3(a), (b), and (c), respectively.

Figure 3(a) shows that for each of the three different initial errors, the periapsis altitude uncertainty approaches the same value after approximately twenty measurements. As can be seen, after this point all three curves continue to converge to approximately the same terminal value of 2 n. mi.

Figure 3(b) illustrates the RMS range uncertainty at periapsis for the same conditions as that for the altitude uncertainty. As can be seen, the major portion of the total RMS position error lies in the down-range component. Also illustrated is that the down-range error cannot be determined until late in the flight. This trait is characteristic of the information obtained from onboard observations. However, this affects only the arrival time, thus performance is generally good regardless (ref. 5). It should be pointed out that the profile of flight-path angle errors would follow the trend of that of the down-range errors. Therefore, flight-path angle errors would also not be determined until late in flight.

The curves of figure 3(c) represent track uncertainties - the third error component of the total RMS position error. Little need be said about these curves for, as can be seen, they drop quite rapidly and continue at rather low values to the terminal point.

Figure 4 presents, in the same sequence as in figure 3, the results of the same study for measurements at 15-minute intervals. Practically the same conclusions can be drawn from the altitude, range, and track curves of figures 4(a), (b), and (c) as were drawn for figures 3(a), (b), and (c). The only appreciable difference appears in the altitude uncertainty curves. Because of the more frequent measurements, there does appear to be a slightly earlier drop and leveling off in the altitude errors with a convergence between 20 and 30 measurements.

The main conclusions that can be drawn from the comparison of spacecraft periapsis position uncertainties for different initial error values are as follows: (1) RMS altitude errors tend to approach the same value after approximately the same number of measurements in all three cases

and continue to converge to the same terminal value, (2) Down-range errors are not determined until late in the flight and tend to be the largest component in the total RMS position error (however, this affects only arrival time), (3) Measurements made at frequencies of less than one per 30 minutes have little effect on the curve profiles when the initial RMS position and velocity errors are equal to or below 300 n. mi. and 18 fps.

Probe.- Figures 5 and 6 pertain to the probe and present the RMS altitude uncertainty at vacuum periapsis for initial errors of 300 n. mi., 18 fps and 150 n. mi., 9 fps using a measurement interval of 30 and 15 minutes, respectively. The altitude uncertainties are plotted against time to Mars vacuum periapsis. Results from these two cases were deemed sufficient for analysis of the probe altitude uncertainties. Thus, no data pertaining to the third case of initial errors were plotted as were done for the spacecraft.

As was expected, upon investigation of the results presented in figures 5 and 6, it is possible to draw approximately the same conclusions for the probe as those for the spacecraft.

Guidance Results

The results of the guidance analysis for the probe and spacecraft are presented in tables I through VI. The correction times, t_c, given in these tables are measured from the time of separation at the Mars sphere of influence. Tables I and II summarize results for single impulse corrections at the times given; tables III through V summarize results for two midcourse corrections with the time of the second correction corresponding to the times, t_{c2}, given in the tables. Table VI compares FTA guidance and the second type of VTA guidance for the probe assuming a perfect navigation system and no velocity-correction implementation errors.

The FTA results presented in these tables attempt to null all position errors at spacecraft periapsis and probe vacuum periapsis. The VTA results in the tables allow the range error to be free while minimizing the magnitude of the applied correction. (This guidance is referred to as radius of periapsis guidance in reference 4.) The aimpoints

for this guidance are also spacecraft periapsis and probe vacuum periapsis. The results for VTA guidance nulling flight-path angle errors at entry are not presented, except in table VI, because in the presence of the navigation system errors assumed and the guidance correction implementation errors chosen, the results for this type of probe guidance (with an aimpoint at the nominal probe entry altitude) were almost equivalent to the FTA guidance results presented.

No attempt was made in this study to develop an analytical solution to the optimum velocity correction schedule. Development of such a solution requires first that three criteria be satisfied (ref. 5). The first of these criteria states that at the time of each correction the miss has been estimated better than it can be corrected. This criteria cannot be satisfied with the navigation system simulated in this study. The addition of Earth-based radar tracking, coupled with an onboard navigation system such as that used in this note, would enable the first criteria to be satisfied. Simulation of this type of tracking was beyond the scope of this study, but will be considered in a future analysis. However, the ΔV results presented in this study, though non-optimum, are more than adequate for preliminary system design.

The velocity correction implementation errors assumed for the tables presented were a 1-percent proportional error and a 1-degree pointing error. The instrument accuracy assumed was 5 arc seconds, and the Mars radius uncertainty was 2 n. mi.

Spacecraft.- In table I the single correction results for the spacecraft are presented for initial errors at separation of 300 n. mi. and 18 fps and navigation measurements processed at 30- and 15-minute intervals, respectively. Using FTA guidance it appears that a spacecraft periapsis altitude dispersion of 5.6 n. mi. can be obtained for one correction equal to 320 fps (RMS); this correction is applied approximately 1 hour prior to spacecraft periapsis passage (17 hours from Mars SOI). With VTA guidance, and applying the single correction at the same time, an RMS ΔV = 260 fps produces a 5.0-n. mi. spacecraft periapsis altitude dispersion. The range dispersion, however, has increased from 87 to 238 n. mi.

Table II represents single correction results for initial errors at separation of 150 n. mi. and 9 fps processing navigation measurements at 30- and 15-minute intervals, respectively. With FTA guidance, an

RMS ΔV = 152 fps produces a 3.8-n. mi. periapsis altitude dispersion; a single correction executed at the same time using VTA guidance requires 130 fps and produces a 3.6-n.m. periapsis altitude dispersion. It should be noted that the single correction values in table II, with initial errors one-half those in table I, are approximately one-half the values of the single correction values presented in the first two tables. The reason for this is that the first midcourse correction after separation attempts to null the dispersions present in the trajectory at separation and therefore is proportional to these dispersions. Consequently, if the initial dispersions are reduced by a factor of two, then the first correction should also be reduced by the same factor.

Table III illustrates the results of making two midcourse corrections, using either FTA or VTA guidance, with initial errors of 300 n. mi. and 18 fps, and processing navigation measurements at 30- and 15-minute intervals. The first correction was assumed to have been made at 9.0 hours from separation (approximately 9.0 hours, also, from spacecraft periapsis) and required an RMS ΔV = 50 fps. The second correction is assumed to be made at any of the times shown in the tables. To illustrate the advantage of making two corrections rather than one, consider table III(b) (FTA guidance) and assume that the second correction is made 17.0 hours from the Mars SOI (approximately 1 hour prior to periapsis passage). The total RMS ΔV = 50 + 187 = 237 fps with a resulting periapsis dispersion of 4.7 n. mi. If now we consider table I(b) (FTA guidance),a single correction executed 17.0 hours from the Mars SOI requires 320 fps with a resulting dispersion of 5.6 n. mi. Therefore, the two corrections have consumed 83 fps less than the single correction and have reduced the periapsis altitude dispersion by approximately 1.0 n. mi.

To illustrate the advantage of VTA over FTA guidance, again consider table III(b). For FTA guidance, as indicated above, two corrections required a total RMS ΔV = 237 fps with a resulting dispersion of 4.7 n. mi. If VTA guidance were used, the total RMS ΔV would be 50 + 11 = 61 fps with a resulting periapsis altitude dispersion of 4.0 n. mi. It should be noted, however, that this reduction in ΔV has been obtained at the expense of increasing the resulting range error from 82 to 237 n. mi. The range error increase is not considered important because it represents only a few seconds difference in periapsis passage time.

Table IV presents the results for two midcourse corrections when the initial errors at separation are 150 n. mi. and 9 fps; table V presents similar results for initial errors of 75 n. mi. and 4.5 fps. The discussion above, presented for the case of initial errors of 300 n. mi. and 18 fps, would apply equally well to these tables and the resulting total RMS ΔV would necessarily be smaller because of the smaller initial dispersions.

These data on spacecraft dispersions indicate that a minimum of two corrections are required inside the sphere of influence in order to keep ΔV requirements to a minimum. However, the system design should include the capability of executing more than two midcourse corrections. (These comments apply equally well to the probe guidance system.)

Probe.- The single correction results for the probe are also presented in tables I and II, with table I using initial errors of 300 n. mi. and 18 fps and table II using initial errors of 150 n. mi. and 9 fps.

The computation of the RMS flight-path angle dispersions presented in the second to last column of these tables (and tables III through V) were calculated by propagating the dispersion matrix to entry, nulling the range errors, and using the resulting matrix in equation C-10 of reference 1. This is not a mathematically rigorous technique but it does represent a reasonable approximation for computing realistic flight-path angle dispersions at the nominal entry altitude. If the range errors are included, the resulting flight-path angle errors computed will be much larger than those presented in the tables but will not represent the error in flight-path angle at the nominal entry altitude (because of the timing error related to the downrange error in the dispersion matrix).

The RMS vacuum periapsis altitude dispersion (1σ) data presented in these tables (as well as tables V through X) are a measure of the corridor width that can be obtained by the probe guidance system.

Using FTA guidance, the data in these tables indicate that an RMS ΔV = 1716 fps will produce a vacuum periapsis altitude dispersion of 5.4 n. mi. ($\sim$ 32 n. mi. corridor) and flight-path angle dispersion of 1.66° with initial errors at separation of 300 n. mi. and 18 fps.

With initial errors of 150 n. mi. and 9 fps (using FTA guidance) a single correction of 811 fps (RMS) is required to produce a vacuum periapsis altitude dispersion of 3.6 n. mi. ($\sim$ 21 n. mi. corridor) and a flight-path angle dispersion of 0.85°. The timing of each of these corrections is 17.5 hours after separation or approximately 20 minutes before the probe arrives at the nominal entry altitude. If VTA guidance for the probe is used (e.g., VTA such that the magnitude of the correction is minimized), the value of the correction is smaller and the vacuum periapsis altitude dispersion is less, but the flight-path angle dispersion at entry is slightly larger. The reason for this is that the VTA guidance allows the range error to be free, and it is precisely the increase in this error which raises the value of the flight-path angle dispersion.

(If VTA guidance were used for the probe with the constraint that flight-path angle errors at entry be nulled, the results would be practically identical to the results obtained for probe FTA guidance. Therefore, these results are not presented in this note.)

The two midcourse correction results for the probe are presented in tables III through V for navigation measurements processed at 30- and 15-minute intervals and with initial errors at separation of 300 n. mi. and 18 fps, 150 n. mi. and 9 fps, and 75 n. mi. and 4.5 fps.

To illustrate the advantage of two corrections over one for probe guidance, consider tables I(b) and III(b) (FTA guidance). In table I(b), as indicated above, a single RMS ΔV = 1716 fps produces a 5.4-n. mi. vacuum periapsis dispersion and a 1.66° flight-path angle dispersion. In table III(b), if the second correction is made at the same time as the single correction cited in table I(b), the total RMS ΔV = 55 + 1073 = 1128 fps with a resulting vacuum periapsis altitude dispersion of 4.5 n. mi. (27 n. mi. corridor width) and a 0.37° flight-path angle dispersion at entry. The two corrections require 588 fps less than the single correction and produce smaller vacuum periapsis altitude and flight-path angle dispersions.

If VTA guidance were used for the probe, the RMS ΔV requirements and corridor width would be decreased, but the flight-path angle dispersions at entry would be increased. As an example consider table III(b) for the probe under VTA guidance. The RMS ΔV = 55 + 55 = 110 fps with a resulting RMS vacuum periapsis altitude dispersion of 3.6 n. mi. ($\sim$ 21 n. mi. corridor width) and a 0.78° flight-path angle dispersion at entry.

The RMS corrections using FTA guidance with the smaller initial errors at separation (see tables III through V) will of course be proportionately smaller and will produce somewhat smaller dispersions at the aimpoints of interest. Likewise, the VTA corrections are smaller than the FTA corrections for the probe, but produce slightly larger flight-path angle dispersions at entry.

Table VI compares probe RMS ΔV and dispersions at vacuum periapsis and entry when using FTA guidance and VTA guidance nulling flight-path angle errors at entry. The first part of the table illustrates what has been already pointed out, that in the presence of the navigation and guidance system errors assumed in this study the FTA and VTA (nulling flight-path angle dispersions) for the probe produce almost identical answers. The two guidance types are compared again at the bottom of the table with zero navigation and guidance correction implementation errors. This data is presented only to illustrate the difference in the constraints imposed by the two guidance laws.

CONCLUDING REMARKS

A comparison of fixed and variable time of arrival guidance for a Mars probe launched from a manned flyby spacecraft has been presented. The problem was initiated with the probe and spacecraft separation at the Mars sphere of influence and was terminated with the probe arrival at a specified entry altitude and the spacecraft arrival at periapsis.

The results of the study indicate that variable time of arrival guidance produces smaller RMS velocity corrections than fixed time of arrival guidance, and would be more advantageous for spacecraft maneuvers. Spacecraft periapsis altitude dispersions of the order of 5.0 n. mi. can be obtained for a single VTA correction of 260 fps when the initial errors at separation are 300 n. mi. and 18 fps. With two midcourse corrections, using VTA guidance, spacecraft periapsis altitude dispersions of 2.6 n. mi. can be obtained for a total RMS ΔV = 75 fps. These numbers are reduced when the initial errors are decreased.

Fixed time of arrival guidance appears to be better for the probe maneuvers in order to more efficiently control the flight-path angle dispersions at entry. With a single FTA correction of 1716 fps, a probe vacuum periapsis altitude dispersion of 5.4 n. mi. (corresponding to a 32.4-n. mi. corridor width) and a flight-path angle dispersion at entry of 1.66° can be obtained with initial errors of 300 n. mi. and 18 fps. With two midcourse corrections, using FTA guidance, a probe vacuum periapsis altitude of 4.5 n. mi. (27-n. mi. corridor width) and flight-path angle dispersion of 0.37° can be achieved for a total RMS ΔV = 1128 fps. These numbers are also proportional to the initial dispersions assumed at the time of separation.

TABLE I.- ACCURACY OBTAINED USING ONE MIDCOURSE CORRECTION AND ASSUMING A 300- N.MI. POSITION ERROR AND AN 18- FPS VELOCITY ERROR AT THE MARS SOI

(a) Navigation measurements processed at 30- minute intervals

GUIDANCE SCHEME	SPACECRAFT				PROBE				
	TIME OF SINGLE CORRECTION, t_{C1}, MEASURED FROM MARS SOI, HR	RMS VELOCITY CORRECTION, FPS	RMS PERIAPSIS ALTITUDE DISPERSION, N. MI.	RMS PERIAPSIS RANGE DISPERSION, N. MI.	TIME OF SINGLE CORRECTION, t_{C1}, MEASURED FROM MARS SOI, HR	RMS VELOCITY CORRECTION, FPS	RMS VACUUM PERIAPSIS ALTITUDE DISPERSION, N. MI.	RMS FLIGHT-PATH ANGLE DISPERSION AT ENTRY, DEG	RMS RANGE DISPERSION AT ENTRY, N. MI.
FIXED-TIME-OF-ARRIVAL GUIDANCE	9.0	50	13.5	238	9.0	55	12.6	0.80	225
	12.0	72	8.3	237	14.0	125	7.1	0.80	222
	17.0	288	7.5	188	17.5	1721	5.8	1.66	76
VARIABLE-TIME-OF-ARRIVAL GUIDANCE	9.0	50	13.5	238	9.0	55	12.6	0.80	225
	12.0	71	8.2	238	14.0	124	7.1	0.81	225
	17.0	260	7.2	238	17.5	1346	5.1	1.75	226

TABLE I.- ACCURACY OBTAINED USING ONE MIDCOURSE CORRECTION AND ASSUMING A 300- N.MI. POSITION ERROR AND AN 18- FPS VELOCITY ERROR AT THE MARS SOI- Concluded

(b) Navigation measurements processed at 15- minute intervals

GUIDANCE SCHEME	SPACECRAFT				PROBE				
	TIME OF SINGLE CORRECTION, t_{C1}, MEASURED FROM MARS SOI, HR	RMS VELOCITY CORRECTION, FPS	RMS PERIAPSIS ALTITUDE DISPERSION, N. MI.	RMS PERIAPSIS RANGE DISPERSION, N. MI.	TIME OF SINGLE CORRECTION, t_{C1}, MEASURED FROM MARS SOI, HR	RMS VELOCITY CORRECTION, FPS	RMS VACUUM PERIAPSIS ALTITUDE DISPERSION, N. MI.	RMS FLIGHT-PATH ANGLE DISPERSION AT ENTRY, DEG	RMS RANGE DISPERSION AT ENTRY, N. MI.
FIXED-TIME-OF-ARRIVAL-GUIDANCE	9.0	50	9.8	238	9.0	55	9.2	0.80	225
	12.0	72	7.0	235	14.0	129	6.4	0.75	208
	17.0	320	5.6	87	17.5	1716	5.4	1.66	82
VARIABLE-TIME-OF-ARRIVAL GUIDANCE	9.0	50	9.8	238	9.0	55	9.2	0.80	225
	12.0	71	6.9	238	14.0	124	6.3	0.81	225
	17.0	260	5.0	238	17.5	1346	4.7	1.75	226

TABLE II.- ACCURACY OBTAINED USING ONE MIDCOURSE CORRECTION AND ASSUMING A 150- N.MI. POSITION ERROR AND A 9- FPS VELOCITY ERROR AT THE MARS SOI

(a) Navigation measurements processed at 30- minute intervals

GUIDANCE SCHEME	SPACECRAFT				PROBE				
	TIME OF SINGLE CORRECTION, t_{C1}, MEASURED FROM MARS SOI, HR	RMS VELOCITY CORRECTION, FPS	RMS PERIAPSIS ALTITUDE DISPERSION, N. MI.	RMS PERIAPSIS RANGE DISPERSION, N. MI.	TIME OF SINGLE CORRECTION, t_{C1}, MEASURED FROM MARS SOI, HR	RMS VELOCITY CORRECTION, FPS	RMS VACUUM PERIAPSIS ALTITUDE DISPERSION, N. MI.	RMS FLIGHT-PATH ANGLE DISPERSION AT ENTRY, DEG	RMS RANGE DISPERSION AT ENTRY, N. MI.
FIXED-TIME-OF-ARRIVAL GUIDANCE	9.0	25	12.4	119	9.0	27	11.5	0.40	112
	12.0	36	6.6	119	14.0	62	5.1	0.40	112
	17.0	135	4.5	111	17.5	818	4.0	0.85	65
VARIABLE-TIME-OF-ARRIVAL GUIDANCE	9.0	25	12.4	119	9.0	27	11.5	0.40	112
	12.0	36	6.5	119	14.0	62	5.1	0.40	112
	17.0	130	4.5	119	17.5	672	3.8	0.88	113

TABLE II.- ACCURACY OBTAINED USING ONE MIDCOURSE CORRECTION AND ASSUMING A 150- N.MI. POSITION ERROR AND A 9- FPS VELOCITY ERROR AT THE MARS SOI- Concluded

(b) Navigation measurements processed at 15- minute intervals

GUIDANCE SCHEME	SPACECRAFT				PROBE				
	TIME OF SINGLE CORRECTION, t_{C1}, MEASURED FROM MARS SOI, HR	RMS VELOCITY CORRECTION, FPS	RMS PERIAPSIS ALTITUDE DISPERSION, N. MI.	RMS PERIAPSIS RANGE DISPERSION, N. MI.	TIME OF SINGLE CORRECTION, t_{C1}, MEASURED FROM MARS SOI, HR	RMS VELOCITY CORRECTION, FPS	RMS VACUUM PERIAPSIS ALTITUDE DISPERSION, N. MI.	RMS FLIGHT-PATH ANGLE DISPERSION AT ENTRY, DEG	RMS RANGE DISPERSION AT ENTRY, N. MI.
FIXED-TIME-OF-ARRIVAL GUIDANCE	9.0	25	8.8	119	9.0	27	8.1	0.40	112
	12.0	36	5.0	119	14.0	63	3.9	0.40	110
	17.0	152	3.8	74	17.5	811	3.6	0.85	68
VARIABLE-TIME-OF-ARRIVAL GUIDANCE	9.0	25	8.8	119	9.0	27	8.1	0.40	112
	12.0	36	5.0	119	14.0	62	3.9	0.40	112
	17.0	130	3.6	119	17.5	672	3.4	0.88	113

TABLE III.- ACCURACY OBTAINED USING TWO MIDCOURSE CORRECTIONS AND ASSUMING A 300- N.MI. POSITION ERROR AND AN 18- FPS VELOCITY ERROR AT THE MARS SOI[a]

(a) Navigation measurements processed at 30- minute intervals

GUIDANCE SCHEME	SPACECRAFT				PROBE				
	TIME OF SECOND CORRECTION, t_{C2}, MEASURED FROM MARS SOI, HR	RMS VELOCITY CORRECTION, FPS	RMS PERIAPSIS ALTITUDE DISPERSION, N. MI.	RMS PERIAPSIS RANGE DISPERSION, N. MI.	TIME OF SECOND CORRECTION, t_{C2}, MEASURED FROM MARS SOI, HR	RMS VELOCITY CORRECTION, FPS	RMS VACUUM PERIAPSIS ALTITUDE DISPERSION, N. MI.	RMS FLIGHT-PATH ANGLE DISPERSION AT ENTRY, DEG	RMS RANGE DISPERSION AT ENTRY, N. MI.
FIXED-TIME-OF-ARRIVAL-GUIDANCE	12.0	7	8.0	237	14.0	18	6.5	0.79	221
	17.0	143	6.7	166	16.0	128	6.4	0.62	171
	18.0	440	4.6	52	17.5	817	6.3	0.61	156
VARIABLE-TIME-OF-ARRIVAL GUIDANCE	12.0	4	8.0	238	14.0	7	6.5	0.80	225
	17.0	15	6.4	238	16.0	14	6.2	0.80	225
	18.0	35	3.7	237	17.5	75	5.9	0.81	225

[a]TIME OF FIRST CORRECTION, t_{C1}, WAS 9.0 HOURS FROM MARS SOI AND REQUIRED A RMS VELOCITY CORRECTION OF 50 FPS FOR THE SPACECRAFT AND 55 FPS FOR THE PROBE.

TABLE III. - ACCURACY OBTAINED USING TWO MIDCOURSE CORRECTIONS AND ASSUMING A 300- N.MI. POSITION ERROR AND AN 18- FPS VELOCITY ERROR AT THE MARS SOI[a] - Concluded

(b) Navigation measurements processed at 15- minute intervals

GUIDANCE SCHEME	SPACECRAFT				PROBE				
	TIME OF SECOND CORRECTION, t_{C2}, MEASURED FROM MARS SOI, HR	RMS VELOCITY CORRECTION, FPS	RMS PERIAPSIS ALTITUDE DISPERSION, N. MI.	RMS PERIAPSIS RANGE DISPERSION, N. MI.	TIME OF SECOND CORRECTION, t_{C2}, MEASURED FROM MARS SOI, HR	RMS VELOCITY CORRECTION, FPS	RMS VACUUM PERIAPSIS ALTITUDE DISPERSION, N. MI.	RMS FLIGHT-PATH ANGLE DISPERSION AT ENTRY, DEG	RMS RANGE DISPERSION AT ENTRY, N. MI.
FIXED-TIME-OF-ARRIVAL GUIDANCE	12.0	8	6.6	235	14.0	36	5.8	0.74	207
	17.0	187	4.7	82	16.0	140	5.6	0.57	157
	18.0	445	3.8	34	17.5	1073	4.5	0.37	73
VARIABLE-TIME-OF-ARRIVAL GUIDANCE	12.0	3	6.6	238	14.0	5	5.8	0.80	225
	17.0	11	4.0	237	16.0	10	5.3	0.80	225
	18.0	25	2.6	237	17.5	55	3.6	0.78	225

[a]TIME OF FIRST CORRECTION, t_{C1}, WAS 9.0 HOURS FROM MARS SOI AND REQUIRED A RMS VELOCITY CORRECTION OF 50 FPS FOR THE SPACECRAFT AND 55 FPS FOR THE PROBE.

TABLE IV.- ACCURACY OBTAINED USING TWO MIDCOURSE CORRECTIONS AND ASSUMING A 150- N.MI. POSITION ERROR AND A 9- FPS VELOCITY ERROR AT THE MARS SOI[a]

(a) Navigation measurements processed at 30- minute intervals

GUIDANCE SCHEME	SPACECRAFT				PROBE				
	TIME OF SECOND CORRECTION, t_{C2}, MEASURED FROM MARS SOI, HR	RMS VELOCITY CORRECTION, FPS	RMS PERIAPSIS ALTITUDE DISPERSION, N. MI.	RMS PERIAPSIS RANGE DISPERSION, N. MI.	TIME OF SECOND CORRECTION, t_{C2}, MEASURED FROM MARS SOI, HR	RMS VELOCITY CORRECTION, FPS	RMS VACUUM PERIAPSIS ALTITUDE DISPERSION, N. MI.	RMS FLIGHT-PATH ANGLE DISPERSION AT ENTRY, DEG	RMS RANGE DISPERSION AT ENTRY, N. MI.
FIXED-TIME-OF-ARRIVAL GUIDANCE	12.0	4	6.6	119	14.0	8	4.7	0.40	112
	17.0	49	4.3	105	16.0	42	4.0	0.37	102
	18.0	209	3.6	47	17.5	276	4.0	0.38	99
VARIABLE-TIME-OF-ARRIVAL GUIDANCE	12.0	4	6.6	119	14.0	6	4.7	0.40	112
	17.0	15	4.3	119	16.0	14	4.0	0.40	112
	18.0	32	3.3	119	17.5	72	3.9	0.42	112

[a] TIME OF FIRST CORRECTION, t_{C1}, WAS 9.0 HOURS FROM MARS SOI AND REQUIRED A RMS VELOCITY CORRECTION OF 25 FPS FOR THE SPACECRAFT AND 27 FPS FOR THE PROBE.

TABLE IV.- ACCURACY OBTAINED USING TWO MIDCOURSE CORRECTIONS AND ASSUMING A 150- N.MI. POSITION ERROR AND A 9- FPS VELOCITY ERROR AT THE MARS SOI[a] - Concluded

(b) Navigation measurements processed at 15-minute intervals

GUIDANCE SCHEME	SPACECRAFT				PROBE				
	TIME OF SECOND CORRECTION, t_{C2}, MEASURED FROM MARS SOI, HR	RMS VELOCITY CORRECTION, FPS	RMS PERIAPSIS ALTITUDE DISPERSION, N. MI.	RMS PERIAPSIS RANGE DISPERSION, N. MI.	TIME OF SECOND CORRECTION, t_{C2}, MEASURED FROM MARS SOI, HR	RMS VELOCITY CORRECTION, FPS	RMS VACUUM PERIAPSIS ALTITUDE DISPERSION, N. MI.	RMS FLIGHT-PATH ANGLE DISPERSION AT ENTRY, DEG	RMS RANGE DISPERSION AT ENTRY, N. MI.
FIXED-TIME-OF-ARRIVAL GUIDANCE	12.0	3	4.9	118	14.0	11	3.6	0.39	110
	17.0	82	3.4	68	16.0	47	3.5	0.35	99
	18.0	218	2.6	32	17.5	480	3.2	0.26	61
VARIABLE-TIME-OF-ARRIVAL GUIDANCE	12.0	3	4.9	119	14.0	5	3.6	0.40	112
	17.0	10	3.3	119	16.0	10	3.4	0.40	112
	18.0	22	2.3	119	17.5	50	2.9	0.40	112

[a]TIME OF FIRST CORRECTION, t_{C1}, WAS 9.0 HOURS FROM MARS SOI AND REQUIRED A RMS VELOCITY CORRECTION OF 25 FPS FOR THE SPACECRAFT AND 27 FPS FOR THE PROBE.

TABLE V.- ACCURACY OBTAINED USING TWO MIDCOURSE CORRECTIONS AND ASSUMING A 75- N.MI. POSITION ERROR AND A 4.5- FPS VELOCITY ERROR AT THE MARS SOI[a]

(a) Navigation measurements processed at 30- minute intervals

GUIDANCE SCHEME	SPACECRAFT				PROBE				
	TIME OF SECOND CORRECTION, t_{C2}, MEASURED FROM MARS SOI, HR	RMS VELOCITY CORRECTION, FPS	RMS PERIAPSIS ALTITUDE DISPERSION, N. MI.	RMS PERIAPSIS RANGE DISPERSION, N. MI.	TIME OF SECOND CORRECTION, t_{C2}, MEASURED FROM MARS SOI, HR	RMS VELOCITY CORRECTION, FPS	RMS VACUUM PERIAPSIS ALTITUDE DISPERSION, N. MI.	RMS FLIGHT-PATH ANGLE DISPERSION AT ENTRY, DEG	RMS RANGE DISPERSION AT ENTRY, N. MI.
FIXED-TIME-OF-ARRIVAL GUIDANCE	12.0	3	6.0	59	14.0	6	4.0	0.20	56
	17.0	18	2.9	57	16.0	16	2.7	0.19	54
	18.0	90	2.8	38	17.5	98	2.6	0.21	54
VARIABLE-TIME-OF-ARRIVAL GUIDANCE	12.0	3	6.0	59	14.0	6	4.0	0.20	56
	17.0	13	2.9	59	16.0	12	2.7	0.20	56
	18.0	28	2.8	59	17.5	65	2.6	0.22	56

[a]TIME OF FIRST CORRECTION, t_{C1}, WAS 9.0 HOURS FROM MARS SOI AND REQUIRED A RMS VELOCITY CORRECTION OF 12 FPS FOR THE SPACECRAFT AND 13 FPS FOR THE PROBE.

TABLE V.- ACCURACY OBTAINED USING TWO MIDCOURSE CORRECTIONS AND ASSUMING A 75- N.MI. POSITION ERROR AND A 4.5- FPS VELOCITY ERROR AT THE MARS SOI[a] - Concluded

(b) Navigation measurements processed at 15- minute intervals

GUIDANCE SCHEME	SPACECRAFT				PROBE				
	TIME OF SECOND CORRECTION, t_{C2}, MEASURED FROM MARS SOI, HR	RMS VELOCITY CORRECTION, FPS	RMS PERIAPSIS ALTITUDE DISPERSION, N. MI.	RMS PERIAPSIS RANGE DISPERSION, N. MI.	TIME OF SECOND CORRECTION, t_{C2}, MEASURED FROM MARS SOI, HR	RMS VELOCITY CORRECTION, FPS	RMS VACUUM PERIAPSIS ALTITUDE DISPERSION, N. MI.	RMS FLIGHT-PATH ANGLE DISPERSION AT ENTRY, DEG	RMS RANGE DISPERSION AT ENTRY, N. MI.
FIXED-TIME-OF-ARRIVAL GUIDANCE	12.0	2	4.3	59	14.0	5	2.7	0.20	56
	17.0	31	2.5	48	16.0	16	2.3	0.19	54
	18.0	100	2.1	29	17.5	182	2.2	0.17	44
VARIABLE-TIME-OF-ARRIVAL GUIDANCE	12.0	2	4.3	59	14.0	4	2.7	0.20	56
	17.0	10	2.4	59	16.0	9	2.3	0.20	56
	18.0	21	2.0	59	17.5	46	2.2	0.21	56

[a]TIME OF FIRST CORRECTION, t_{C1}, WAS 9.0 HOURS FROM MARS SOI AND REQUIRED A RMS VELOCITY CORRECTION OF 12 FPS FOR THE SPACECRAFT AND 13 FPS FOR THE PROBE.

TABLE VI.-PROBE RMS ΔV SUMMARY COMPARING FTA AND $VTA_{\Delta\gamma_E = 0}$ GUIDANCE WITH AND WITHOUT NAVIGATION AND GUIDANCE CORRECTION IMPLEMENTATION ERRORS[a]

		Time of correction measured from Mars SOI, hr	RMS velocity correction, fps	RMS vacuum periapsis altitude dispersion, n.mi.	RMS flight-path angle dispersion at entry, deg	RMS altitude dispersion at entry, n.mi.	RMS range dispersion at entry, n.mi.	RMS track dispersion at entry, n.mi.
With navigation and guidance correction implementation errors	FTA guidance	9.0	54.47	12.650	6.014	55.3000	225.300	10.320
		17.5	817.50	6.322	4.167	40.7900	156.700	2.354
	$VTA_{\Delta\gamma_E = 0}$ guidance	9.0	54.61	12.670	6.014	55.3000	225.400	10.310
		17.5	832.60	6.688	4.165	40.8300	156.600	2.173
Without navigation and guidance correction implementation errors	FTA guidance	9.0	67.20	1.066	5×10^{-2}	1.2620	0.657	0.810
		17.5	1763.00	1×10^{-3}	1.555	12.9800	14.660	14.550
	$VTA_{\Delta\gamma_E = 0}$ guidance	9.0	67.32	0.499	5×10^{-6}	0.5099	2.276	6×10^{-4}
		17.5	1909.00	13.890	6×10^{-5}	14.3100	63.910	2×10^{-2}

[a]Position and velocity errors at Mars SOI were 300 n. mi. and 18 fps, respectively.

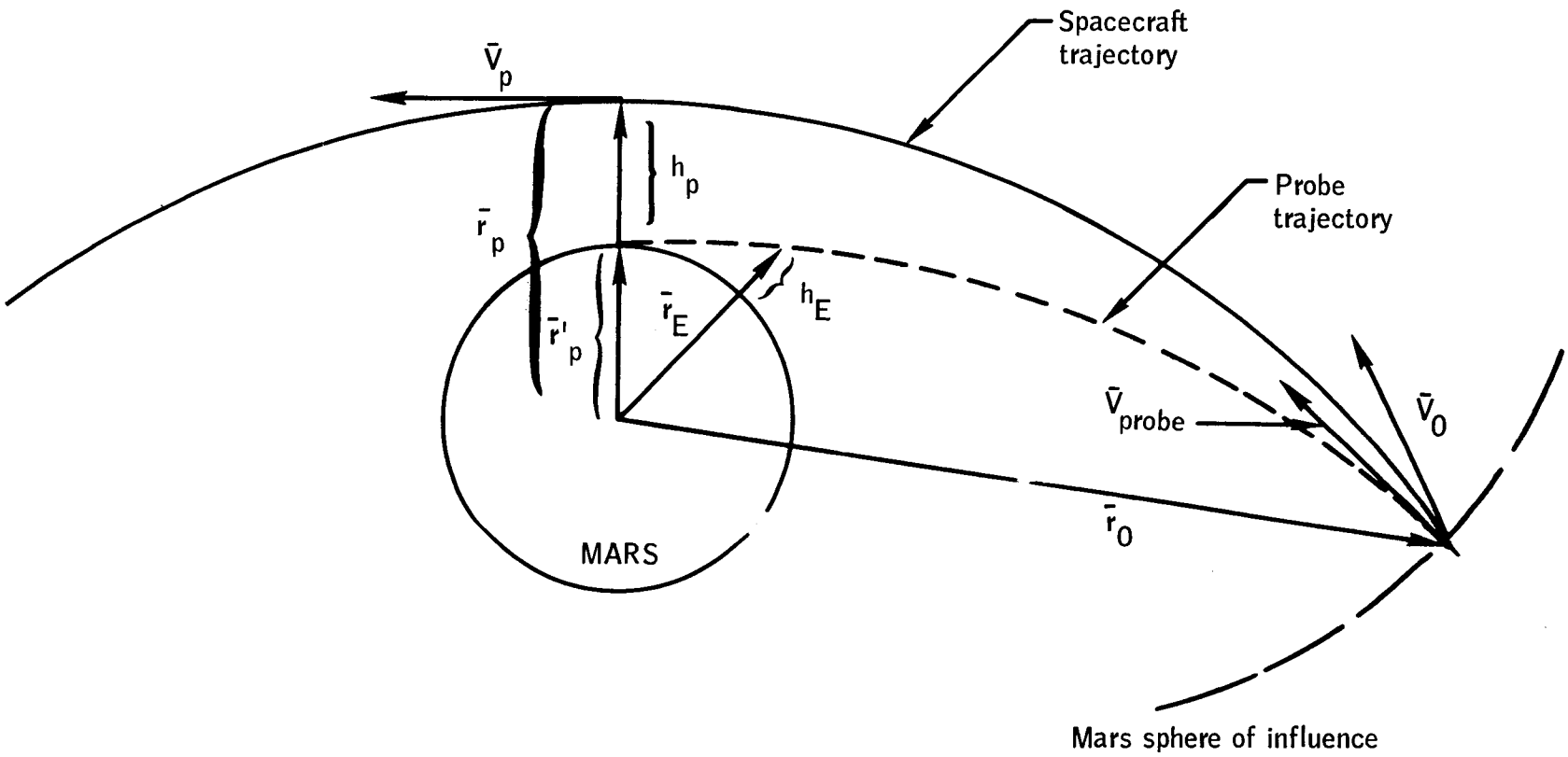

Figure 1. - Probe and spacecraft reference trajectory geometry.

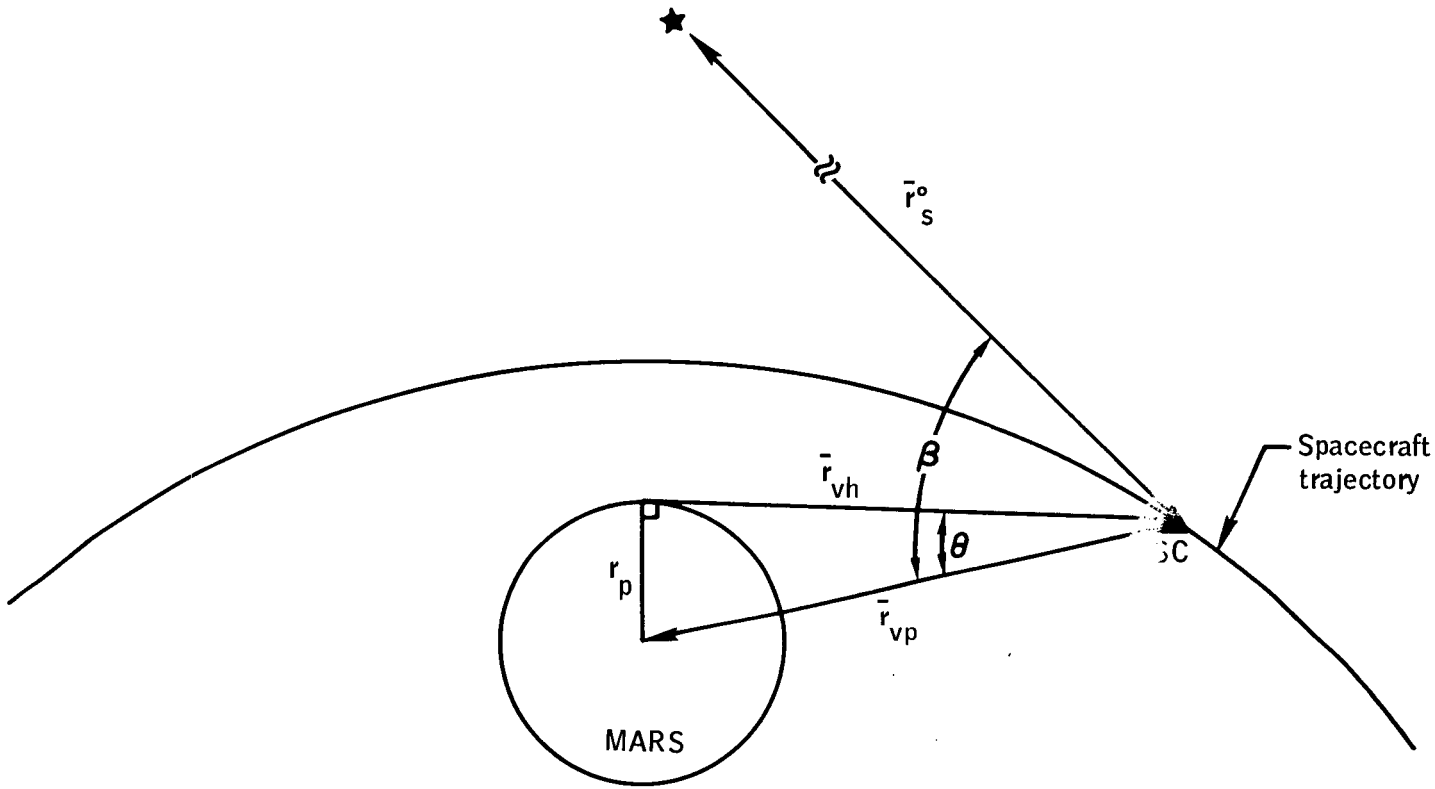

Figure 2.- Geometry of planet-star included angle measurement.

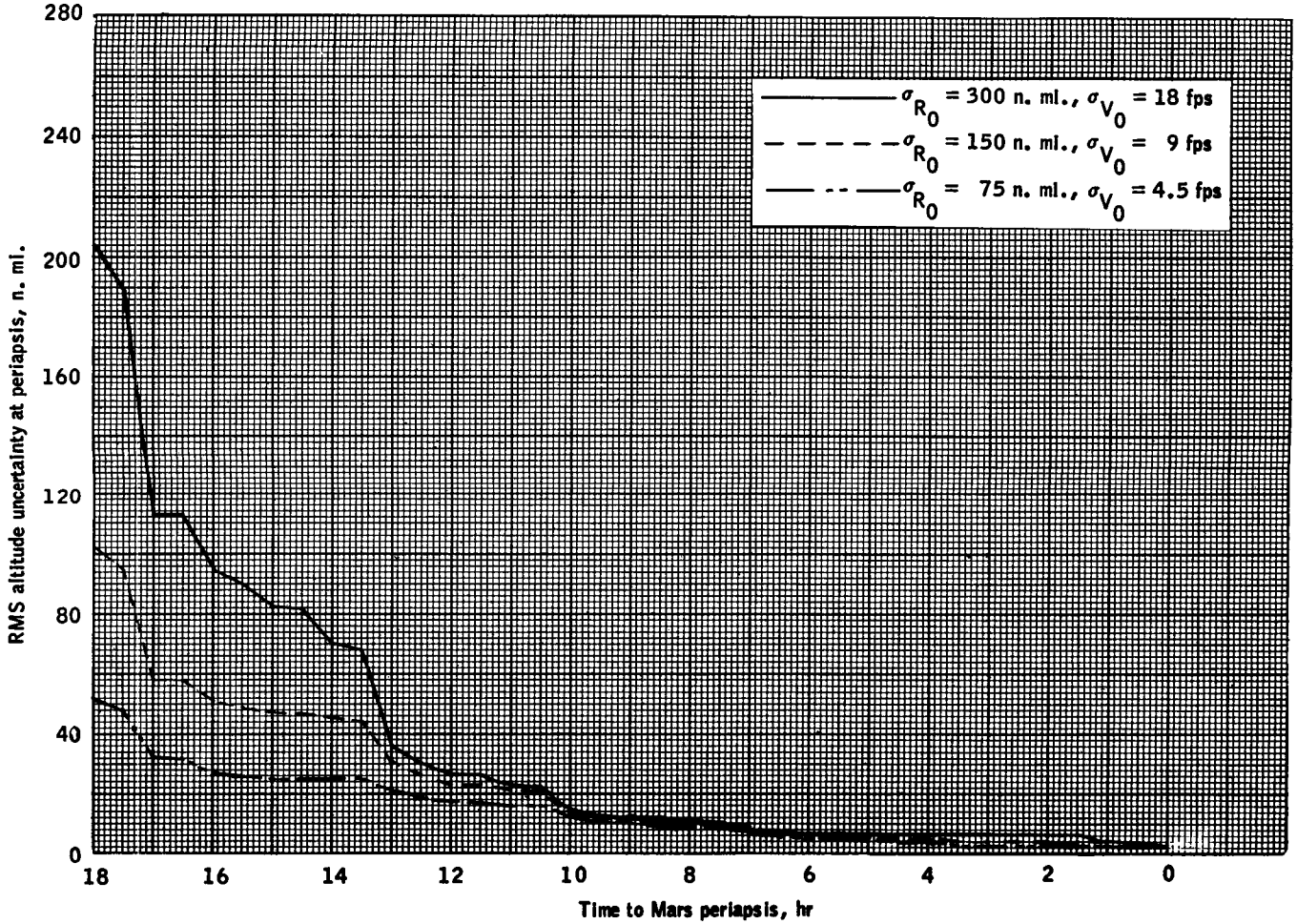

(a) RMS altitude uncertainties at periapsis.

Figure 3.- Spacecraft RMS periapsis position uncertainties for measurement intervals of 30 minutes.

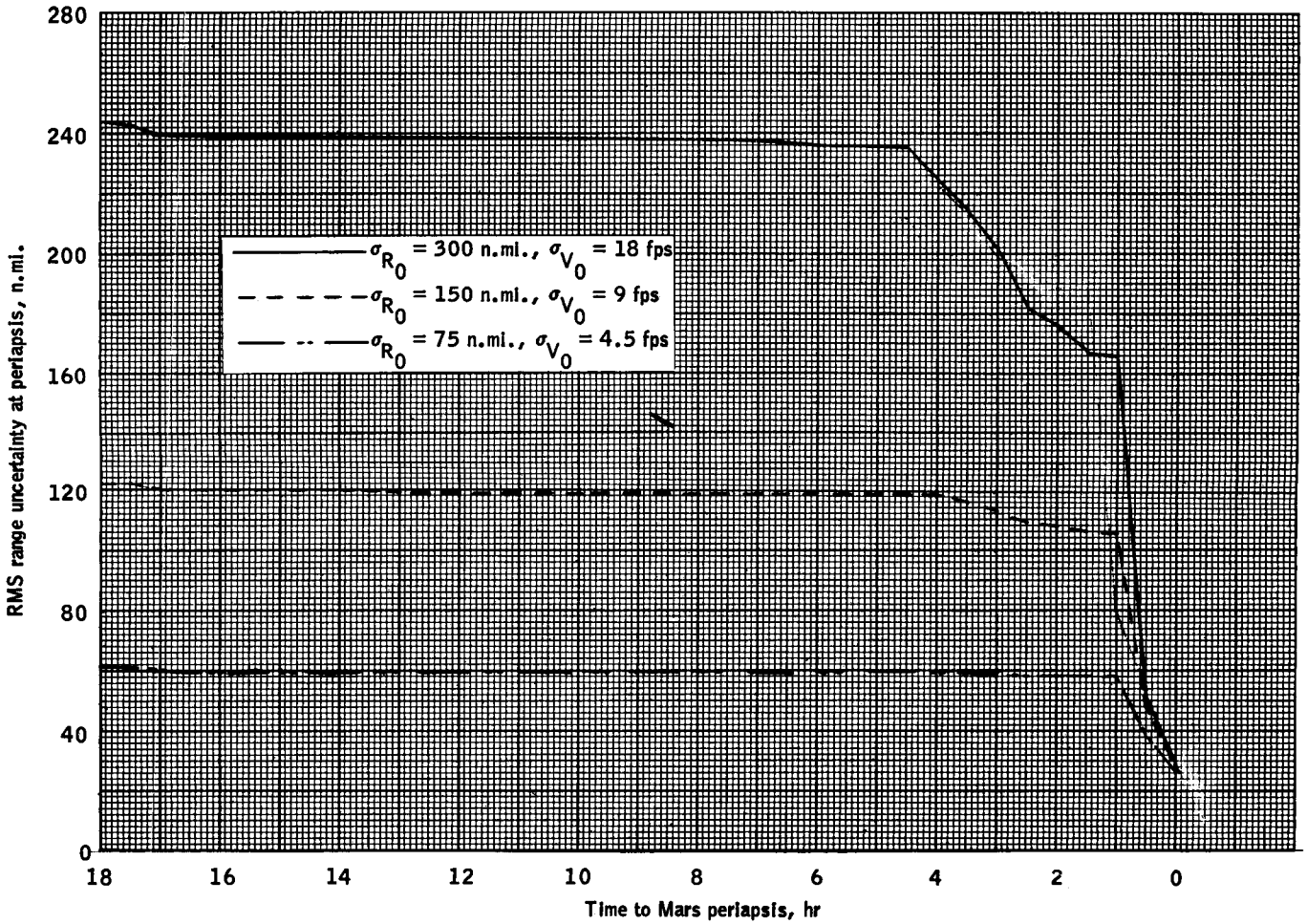

(b) RMS range uncertainties at periapsis.

Figure 3.- Continued.

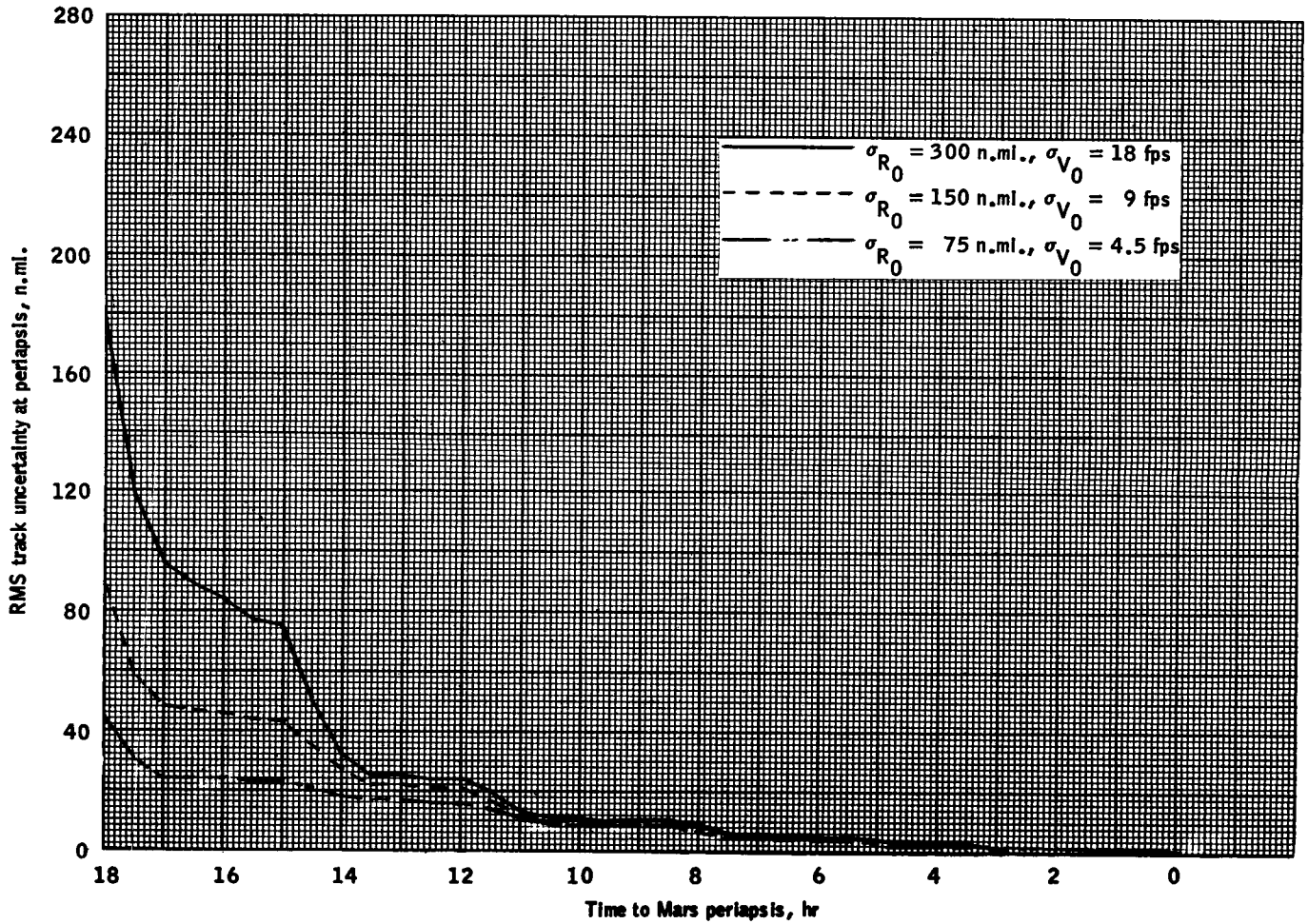

(c) RMS track uncertainties at periapsis.

Figure 3.- Concluded.

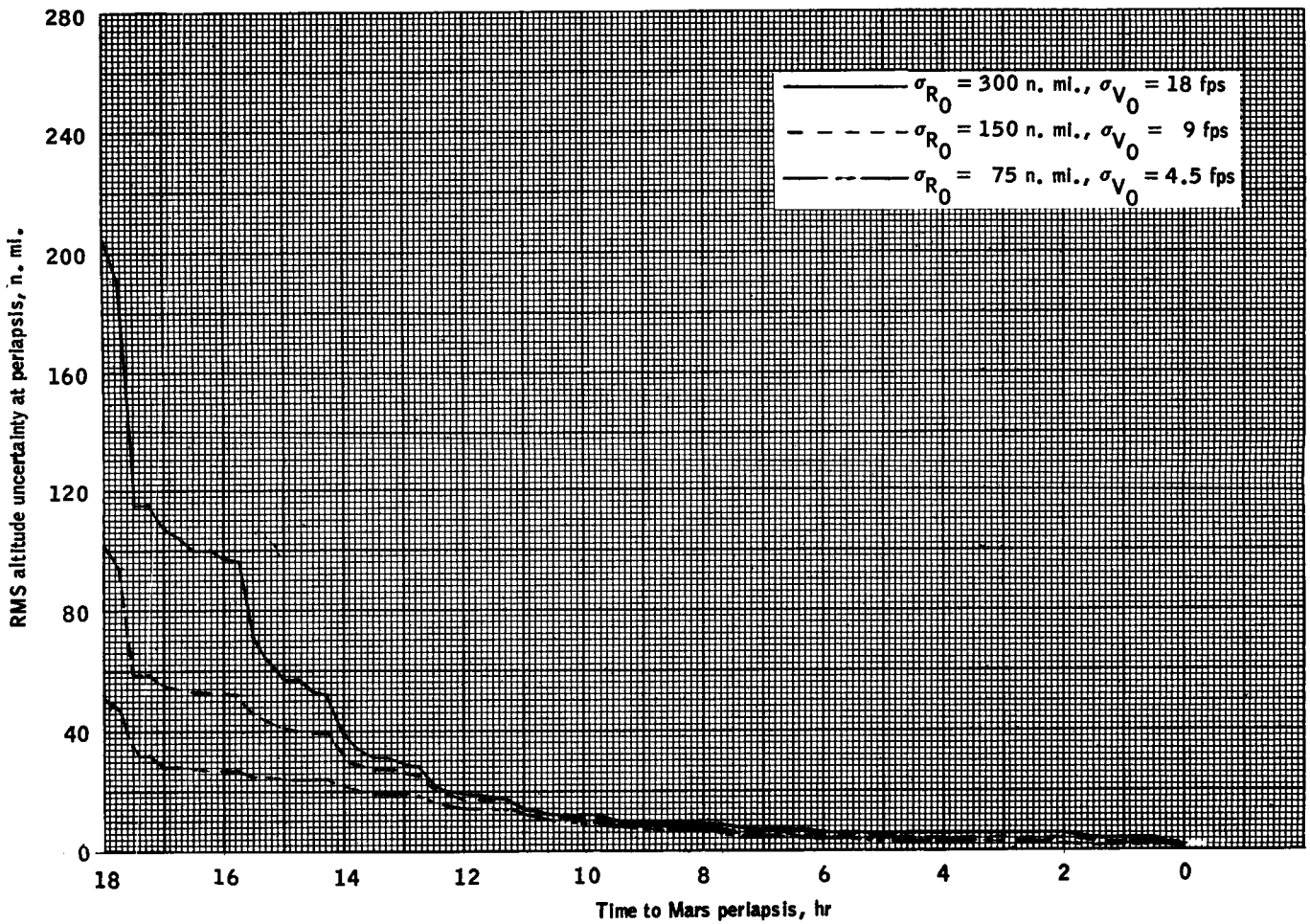

(a) RMS altitude uncertainties at periapsis.

Figure 4.- Spacecraft RMS periapsis position uncertainties for measurement intervals of 15 minutes.

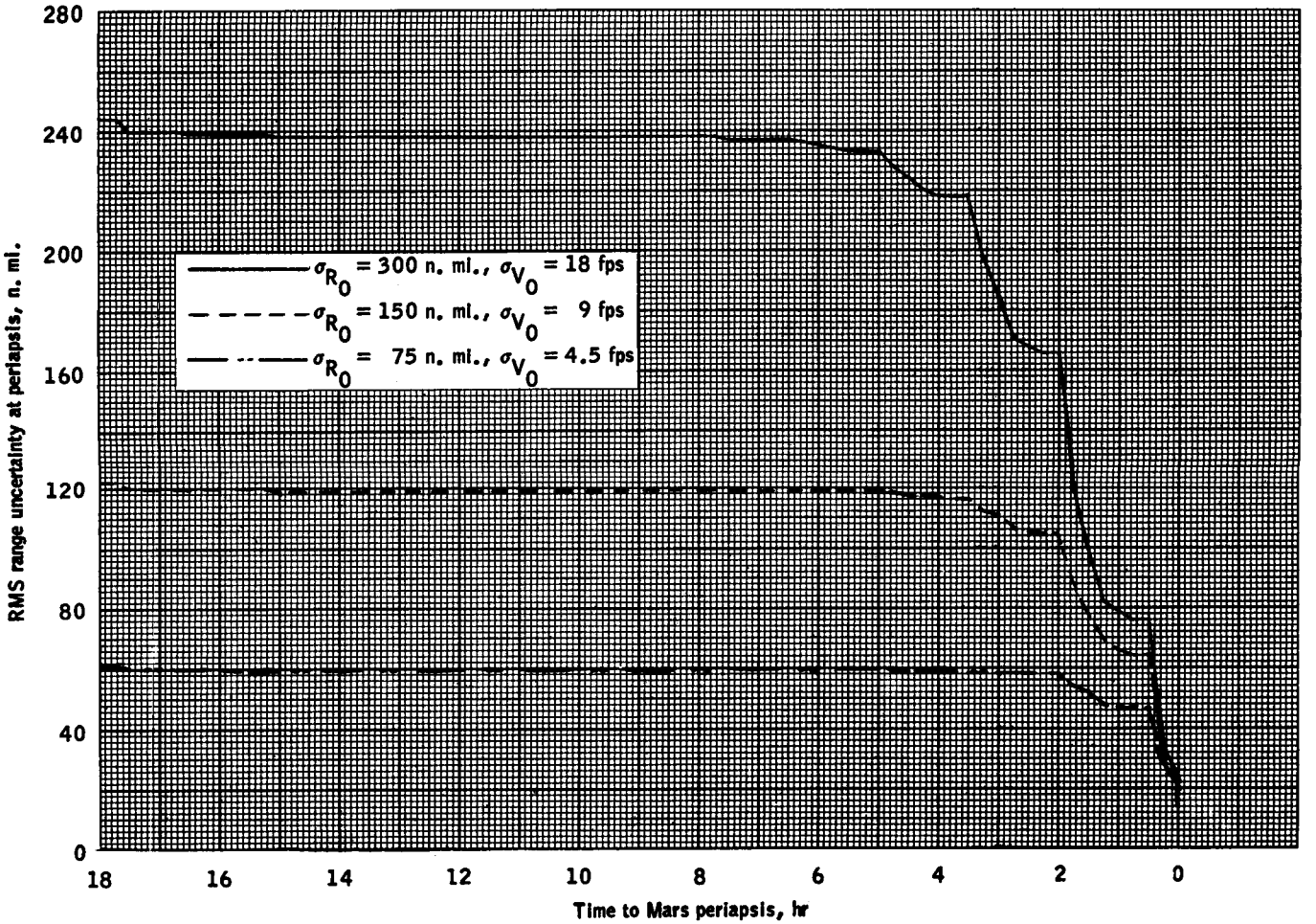

(b) RMS range uncertainties at periapsis.

Figure 4.- Continued.

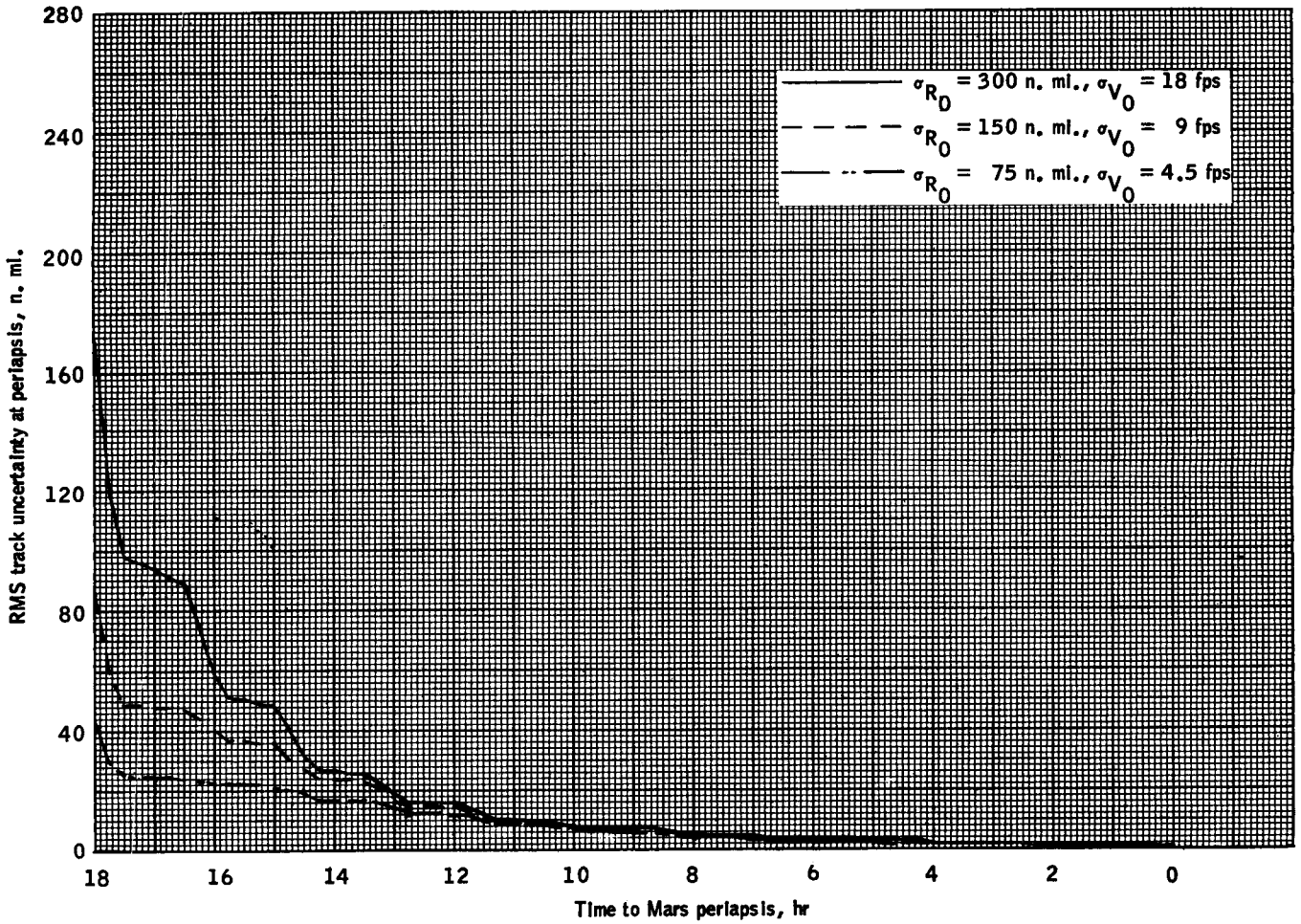

(c) RMS track uncertainties at periapsis.

Figure 4.- Concluded.

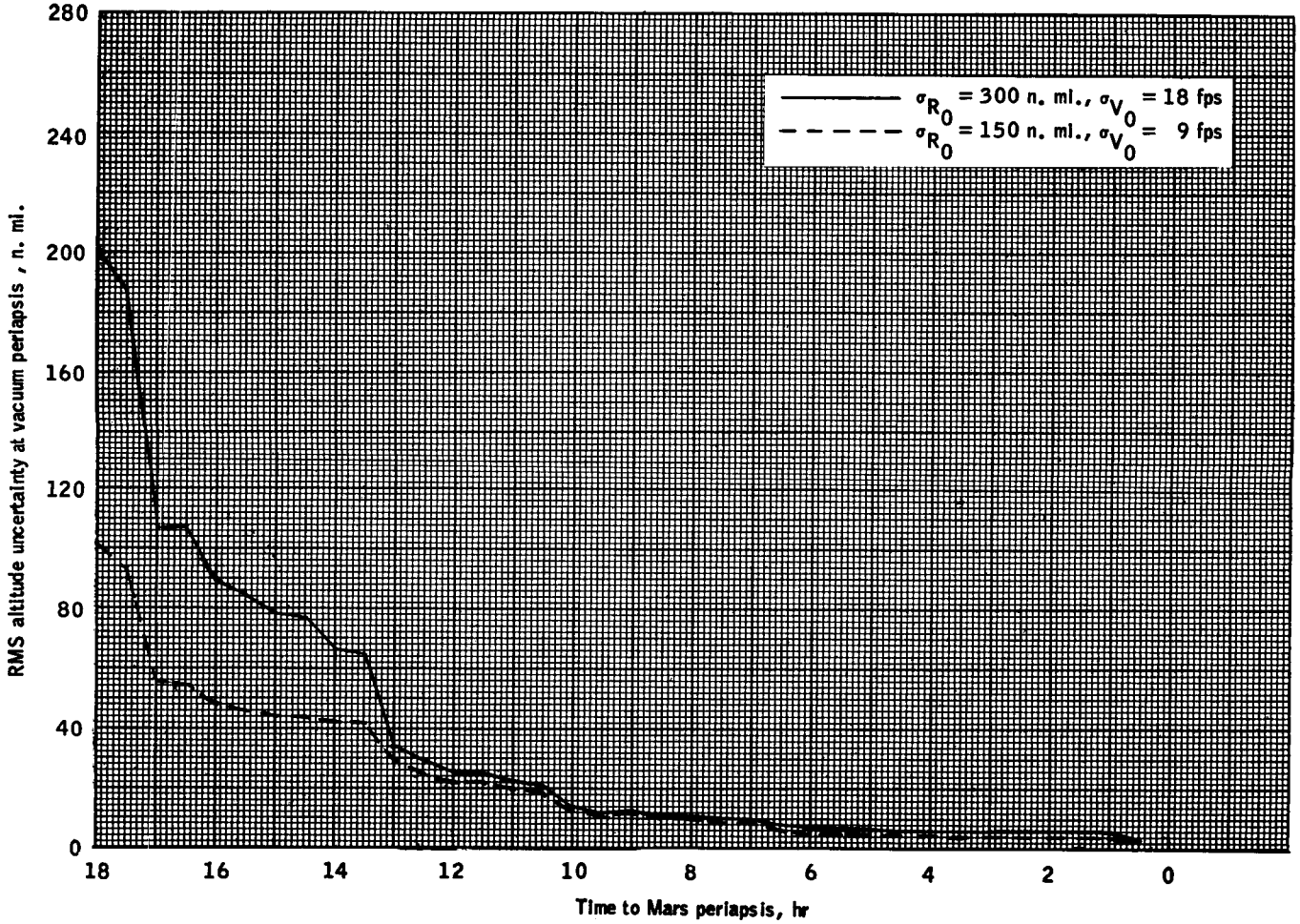

Figure 5.- Probe RMS vacuum periapsis altitude uncertainties for measurement intervals of 30 minutes.

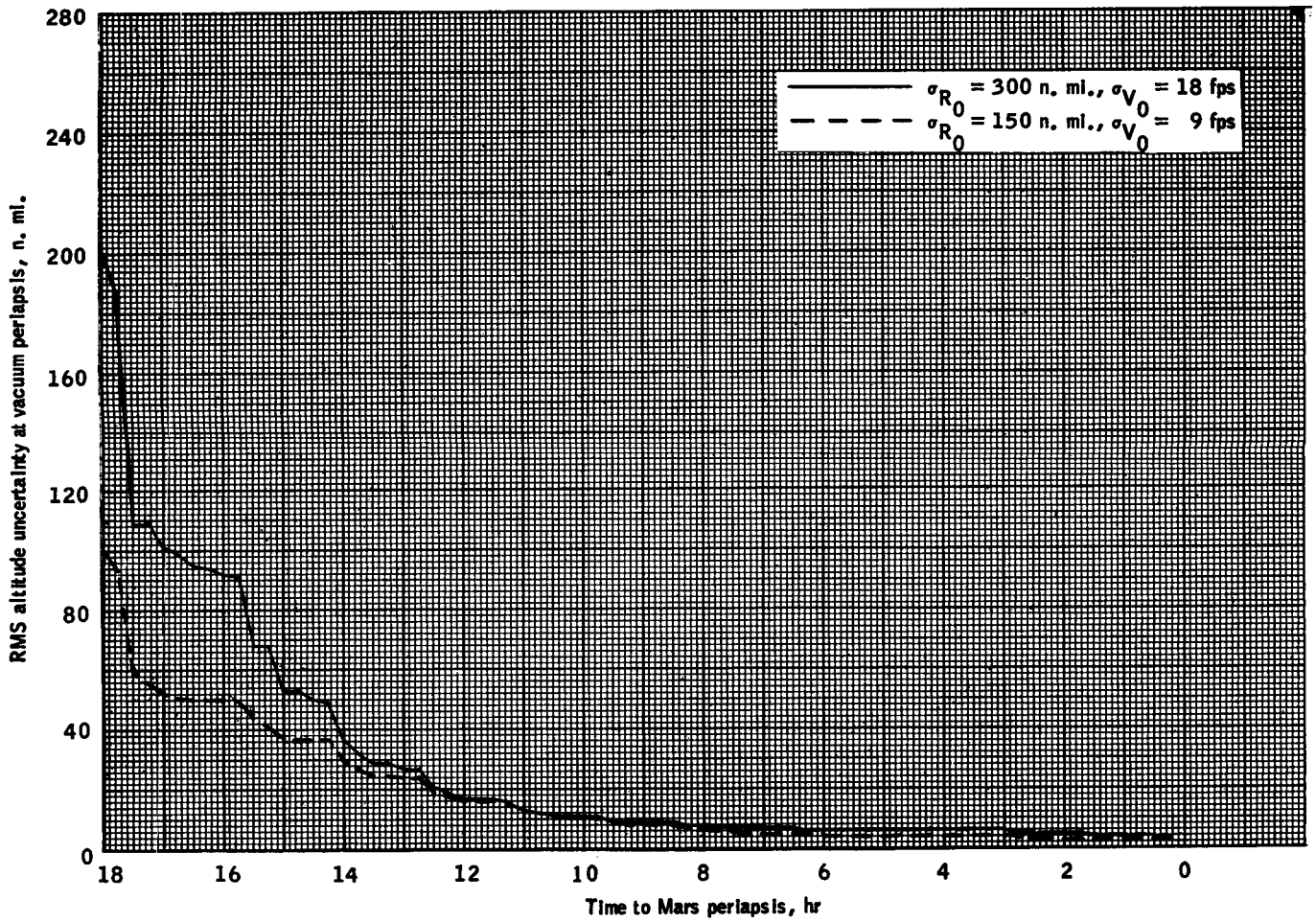

Figure 6.- Probe RMS vacuum periapsis altitude uncertainties for measurement intervals of 15 minutes.

APPENDIX

SOLUTION FOR THE CONIC TRAJECTORY THAT SATISFIES THE TERMINAL ENTRY CONDITIONS OF v_E, γ_E, h_E

It is assumed that the probe is at the initial position vector, $\bar{r}_o$, and it is desired that the terminal or entry speed, v_E, flight-path angle, γ_E, and altitude, h_E, be satisfied. The inclination, i, of the trajectory is also specified. The geometry of this problem is shown in figure A1. The derivation of the velocity required $\bar{v}_R$ ($\bar{v}_R = \bar{v}_{PROBE}$) at t_o to satisfy these conditions will now be derived.

The semi-major axis of the trajectory is computed from,

$$a = \left(\frac{2}{r_E} - \frac{v_E^2}{\mu}\right)^{-1} \tag{A-1}$$

where $r_E = h_E + R_p$. If $a>0$, the trajectory is elliptic; if $a<0$, the trajectory is hyperbolic.

The parameter, p, is found from,

$$p = \frac{v_E^2 \, r_E^2 \, \sin^2(\gamma_E)}{\mu} \tag{A-2}$$

The eccentricity of the trajectory is then,

$$e = \sqrt{1 - \frac{p}{a}} \tag{A-3}$$

The radius of periapsis is found from,

$$r_\pi = a(1 - e) \tag{A-4}$$

At this point it should be noted that if the trajectory is elliptical the constraint

$$r_o \leq 2a - r_\pi \tag{A-5}$$

must be imposed.

From the polar equation of the orbit, the angle Θ between $\bar{r}_o$ and entry may be found the true anomalies,

$$f_o = \cos^{-1}\left[\frac{1}{e}\left(\frac{p}{r_o} - 1\right)\right] \tag{A-6}$$

and

$$f_E = \cos^{-1}\left[\frac{1}{e}\left(\frac{p}{r_E} - 1\right)\right] \tag{A-7}$$

and by setting

$$\theta = f_E - f_o \tag{A-8}$$

The normal to the trajectory plane is computed from

$$\hat{h} = \hat{i} \sin \Omega \sin i - \hat{j} \cos \Omega \sin i + \hat{k} \cos i. \tag{A-9}$$

The inclination, i, is specified, and Ω is the right ascension of the ascending node which may be computed from $\bar{r}_o$ and i, except for an ambiguity which may be freely chosen.

From figure A2, the right ascension α_o and declination δ_o of $\bar{r}_o$ may be computed from

$$\alpha_o = \tan^{-1}\left(\frac{y_o}{x_o}\right) \tag{A-10}$$

and

$$\delta_o = \sin^{-1}\left(\frac{z_o}{r_o}\right) \tag{A-11}$$

Also from figure A2,

$$\Omega = \alpha_o - \sigma \tag{A-12}$$

for one choice of Ω

$$\Omega = \alpha_o + \sigma + \pi \tag{A-13}$$

for the other choice of Ω. For both cases, σ is computed from

$$\sin \sigma = \frac{\tan \delta_o}{\tan i} . \tag{A-14}$$

Equation (A-14) implies the limits on inclination which may be specified, that is,

$$\left|\tan i_o\right| > \left|\tan \delta_o\right| \tag{A-15}$$

for (A-14) to be meaningful.

From figure A1, it is evident that the entry position and velocity may be written

$$\bar{r}_E = r_E \left(\cos \theta \frac{\bar{r}_o}{r_o} + \sin \theta \hat{W}\right) \tag{A-16}$$

and

$$\bar{v}_E = v_E \left[\cos \left(\theta + \gamma_T\right) \frac{\bar{r}_o}{r_o} + \sin \left(\theta + \gamma_T\right) \hat{W}\right] \tag{A-17}$$

where the unit vector $\hat{W}$ lies in the trajectory plane and is defined by

$$\hat{W} = \hat{h} \times \frac{\bar{r}_o}{r_o} . \tag{A-18}$$

The velocity required may now be simply found from the triple cross-product

$$\bar{r}_o \times \left(\bar{r}_o \times \bar{v}_R\right) = \bar{r}_o \times \left(\bar{r}_E \times \bar{v}_E\right) \tag{A-19}$$

which is true since $\bar{r}_o \times \bar{v}_R = \bar{r}_E \times \bar{v}_E$ is the angular momentum vector which must remain constant. After considerable algebra (A-19) may be solved for $\bar{v}_R$,

$$\bar{v}_R = \frac{\bar{r}_o}{r_o} v_o \cos \gamma_o + \hat{W} \frac{r_E v_E}{r_o} \sin \gamma_T . \tag{A-20}$$

The magnitude of $\bar{v}_R$ is found from

$$v_R^2 = \mu\left(\frac{2}{r_o} - \frac{1}{a}\right) . \tag{A-21}$$

The initial flight-path angle γ_o may be found from

$$\left|\bar{r}_o \times \bar{v}_R\right| = \left|\bar{r}_E \times \bar{v}_E\right| \tag{A-22}$$

or, $r_o v_R \sin \gamma_o = r_E v_E \sin \gamma_E$

and
$$\gamma_o = \sin^{-1}\left(\frac{r_E v_E \sin \gamma_E}{r_o v_R}\right). \tag{A-23}$$

The time to entry may be computed from the following equation from reference 6:

$$\sqrt{\mu}\, t_E = \frac{\bar{r}_o \cdot \bar{v}_R}{\sqrt{\mu}} X^2 C\left[\alpha X^2\right] + \left[1 - r_o \alpha_o\right] X^3 S\left[\alpha_o X^2\right] + r_o X \tag{A-24}$$

where $\alpha = \frac{1}{a}$ and $C\left[\alpha X^2\right]$ and $S\left[\alpha X^2\right]$ are Battin's auxiliary functions. X is found from

$$X = \left[E_E - E_o\right] \Big/ \sqrt{\alpha}, \text{ if } a>o \tag{A-25}$$

$$X = \left[H_E - H_o\right] \Big/ \sqrt{-\alpha}, \text{ if } a<o \,. \tag{A-26}$$

If the trajectory is elliptical (a>0), the quantities E_E and E_o are the eccentric anomalies and are found from

$$\tan\left(\frac{E}{2}\right) = \sqrt{\frac{1-e}{1+e}} = \tan\left(\frac{f}{2}\right) \tag{A-27}$$

If the trajectory is hyperbolic ($a<0$), the quantities H_E and H_o are found from

$$\tan h\left(\frac{H}{2}\right) = \sqrt{\frac{e-1}{e+1}}\ \tan\left(\frac{f}{2}\right) \tag{A-28}$$

When these equations are applied to determine the $\bar{v}_R$ of the probe, the inclination and right ascension of the ascending node are the same or very nearly the same as that of the spacecraft.

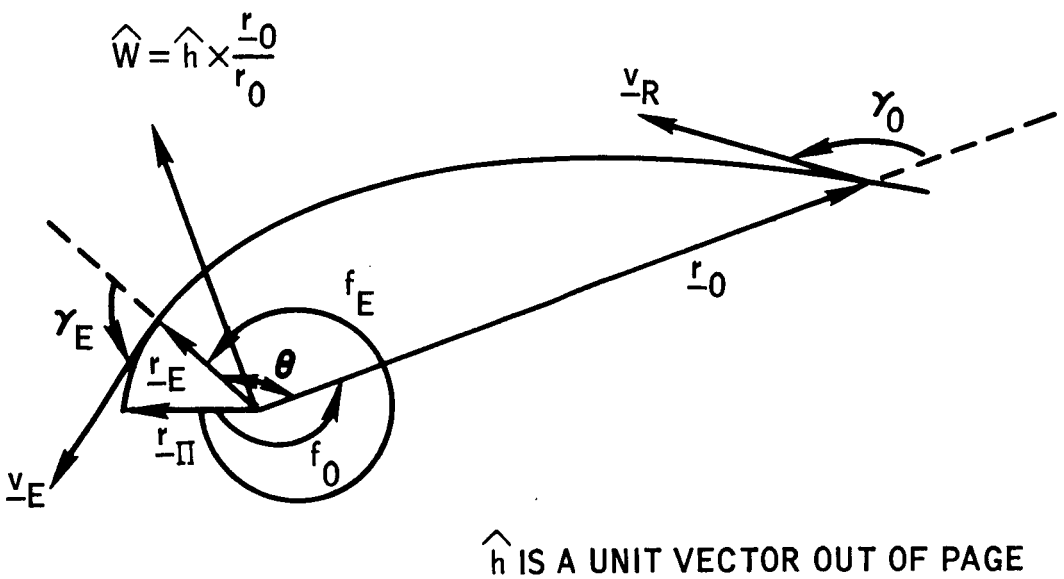

Figure A1.- Geometry of trajectory which satisfies the entry conditions V_E, γ_E, r_E $(= R_p + h_E)$.

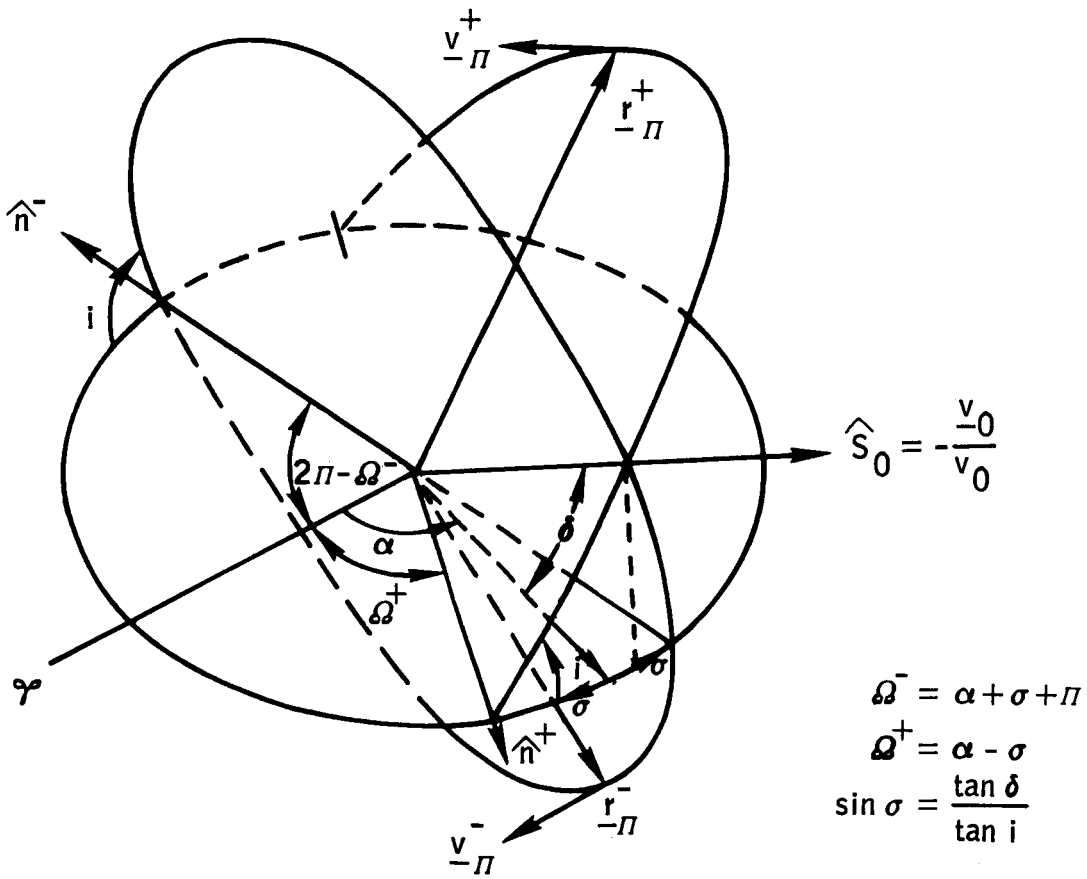

Figure A2.- Geometry of the two trajectories possible that satisfy the entry conditions.

REFERENCES

1. Murtagh, Thomas B.; and Lowes, Flora B.: Preliminary Navigation and Guidance Analysis of a Martian Probe Launched from a Manned Flyby Spacecraft. MSC Internal Note 67-FM-3, January 12, 1967.

2. Bond, Victor R.; and Henry, Ellis W.: One-Way and Flyby Interplanetary Trajectory Approximations Using Matched Conic Techniques. MSC Internal Note 67-FM-16, February 3, 1967.

3. Bond, Victor R.; and Murtagh, Thomas B.: Fixed and Variable Time of Arrival Guidance Matrices for Interplanetary Flight. MSC Internal Note 67-FM-53, April 21, 1967.

4. Cicolani, L. S.: Linear Theory of Impulsive Velocity Corrections for Space Mission Guidance. NASA TN D-3365, April, 1966.

5. Cicolani, L. S.: Interplanetary Midcourse Guidance Using Radar Tracking and On-Board Observation Data. NASA TN D-3623, September, 1966.

6. Battin, R. H.: Astronautical Guidance. McGraw-Hill Book Company, 1964.